Schizophrenia Bulletin vol. 51 no. 3 pp. 804–817, 2025
https://doi.org/10.1093/schbul/sbae150
Advance Access publication September 9, 2024

EEG-based Signatures of Schizophrenia, Depression, and Aberrant Aging: A Supervised Machine Learning Investigation

Elif Sarisik[1–3], David Popovic[1–4], Daniel Keeser[2,4–6], Adyasha Khuntia[2,3], Kolja Schiltz[1], Peter Falkai[1,2,4], Oliver Pogarell[1], and Nikolaos Koutsouleris[1,2,4,6,7,*]

[1]Max Planck Fellow Group Precision Psychiatry, Max Planck Institute of Psychiatry, Munich, Germany; [2]Department of Psychiatry and Psychotherapy, LMU University Hospital, LMU Munich, Munich, Germany; [3]International Max Planck Research School for Translational Psychiatry (IMPRS-TP), Munich, Germany; [4]German Center for Mental Health (DZPG), Partner Site Munich, Munich, Germany; [5]NeuroImaging Core Unit Munich (NICUM), LMU University Hospital, LMU Munich, Munich, Germany; [6]Munich Center for Neurosciences, LMU Munich, Munich, Germany; [7]Institute of Psychiatry, Psychology and Neuroscience, King's College, London, UK

Elif Sarisik and David Popovic are shared first authors. Oliver Pogarell and Nikolaos Koutsouleris are shared last authors.

[*]To whom correspondence should be addressed; Department of Psychiatry and Psychotherapy, Ludwig-Maximilian-University, Nussbaumstr. 7, 80336 Munich, Germany; tel: +49-89-4400-55885, fax: +49-89-4400-44776, e-mail: nikolaos.koutsouleris@med.uni-muenchen.de

***Background*: Electroencephalography (EEG) is a noninvasive, cost-effective, and robust tool, which directly measures in vivo neuronal mass activity with high temporal resolution. Combined with state-of-the-art machine learning (ML) techniques, EEG recordings could potentially yield in silico biomarkers of severe mental disorders. *Hypothesis*: Pathological and physiological aging processes influence the electrophysiological signatures of schizophrenia (SCZ) and major depressive disorder (MDD). *Study Design*: From a single-center cohort ($N = 735$, 51.6% male) comprising healthy control individuals (HC, $N = 245$) and inpatients suffering from SCZ ($N = 250$) or MDD ($N = 240$), we acquired resting-state 19 channel-EEG recordings. Using repeated nested cross-validation, support vector machine models were trained to (1) classify patients with SCZ or MDD and HC individuals and (2) predict age in HC individuals. The age model was applied to patient groups to calculate Electrophysiological Age Gap Estimation (EphysAGE) as the difference between predicted and chronological age. The links between EphysAGE, diagnosis, and medication were then further explored. *Study Results*: The classification models robustly discriminated SCZ from HC (balanced accuracy, BAC = 72.7%, $P < .001$), MDD from HC (BAC = 67.0%, $P < .001$), and SCZ from MDD individuals (BAC = 63.2%, $P < .001$). Notably, central alpha (8–11 Hz) power decrease was the most consistently predictive feature for SCZ and MDD. Higher EphysAGE was associated with an increased likelihood of being misclassified as SCZ in HC and MDD ($\rho_{HC} = 0.23$, $P < .001$; $\rho_{MDD} = 0.17$, $P = .01$). *Conclusions*: ML models can extract electrophysiological signatures of MDD and SCZ for potential clinical use. However, the impact of aging processes on diagnostic separability calls for timely application of such models, possibly in early recognition settings.**

Key words: psychosis spectrum disorders/affective disorders/support vector machine/precision psychiatry/electrophysiology/early intervention

Introduction

Ever since Hans Berger tried to understand "psychic energy" in 1929 electroencephalography (EEG) has been used to measure mass neuronal activity.[1,2] Over the years, both distinct and common EEG patterns for severe mental illnesses (SMIs) were established. Regarding EEG-based quantitative frequency band analysis of resting-state recordings, the increased delta (1–4 Hz) and theta (4–8 Hz) activity, which are theorized as an indicator of generalized slowing of the EEG activity, were found in both schizophrenia (SCZ) and major depressive disorder (MDD)[3–5] and linked to dysfunctional cognitive processing.[6] Furthermore, delta waves constitute the predominant slow rhythms in states of sleep and anesthesia which are unconscious states in

a broader term[7,8] whereas the theta band power is involved in working memory, sensory stimuli perception, and attentional control.[9,10] SCZ patients showed abnormalities in the dominant alpha frequency (8–12 Hz) power indicative of "hypofrontality," a state of diminished cerebral blood flow in the frontal cortex[5,11–13] and in the gamma frequency band (30–100 Hz)[14] which is involved in neuronal synchronization in both local and large scale neuronal networks underlying a large range of perceptual and higher order cognitive functions typically impaired in SCZ.[15–17] Yet, patients with MDD display power changes neither in alpha activity nor beta (12–30 Hz) activity when compared to healthy control (HC) individuals.[5] However, distinct patterns emerge in MDD, characterized by greater alpha activity in frontal regions of the left hemisphere relative to the right hemisphere, a phenomenon known as alpha asymmetry.[18] This alpha asymmetry has been suggested to stem from disrupted emotional processing in MDD.[19] Regarding connectivity, diverging results were found, with some studies reporting increased EEG connectivity in SMI, while others found decreased connectivity.[20,21]

Recent advances in machine learning (ML) and increased computational power have led to renewed interest in EEG techniques as a powerful and cost-effective tool to investigate neurobiological patterns of SMI offering the potential of direct, neuronal biomarkers.[22,23] ML allows to capture complex and distributed patterns of psychiatric disorders[24,25] and has already been successfully employed to detect SMI based on electrophysiological data.[26–30] EEG-based models identified SCZ patients with accuracies above 71%,[31–35] while MDD patients were detected with accuracies up to 89%.[31,36–38] Regarding differential diagnosis between SCZ and MDD, ML models reached accuracies around 60%.[31,39,40] However, there is a strong possibility that these high accuracies may be the result of models being overfitted on small samples.[41] Therefore, strict cross-validation schemes, validation analyses, and thorough assessments of generalizability are needed to examine the translational robustness of such models. Additionally, exploring the underlying neural mechanisms driving these diagnostic patterns could offer valuable insights into the pathophysiology of SMIs and guide the development of more targeted interventions and treatments.

One promising measure of dysfunctional brain development is the "Brain Age Gap Estimation" (BrainAGE). BrainAGE uses supervised ML to build normative aging models, which are first trained to predict age in HC individuals and then applied to patient cohorts yielding a neurobiologically predicted age.[42] BrainAGE is the difference in years between that predicted age and the chronological age, that is, an individualized metric to quantify the acceleration or deceleration of brain structural aging.[43] So far, evidence for increased BrainAGE has been found across SMIs.[44] First-episode psychosis patients show subtler deviations between +1.17 and +3.39 years,[45–49] while SCZ patients show increased BrainAGE ranging from +2.56 to +9.00 years.[43,50–52] In depression, effects are less pronounced, with some studies reporting non-significant results[53,54] and others mentioning BrainAGE scores of up to +4 years.[48,54–56] However, it remains unclear if similar electrophysiological aging processes occur. To date, few studies have explored the potential of EEG in predicting age-related disease processes and produced preliminary models that explain 33%–69% of age variance in HC.[57–60] These changes include variance in delta and theta frequency band powers, reduced power in alpha frequency band, and increased beta band power in older individuals.[61,62]

Therefore, we employed supervised ML to explore electrophysiological patterns of SMI by (1) building and validating (differential) diagnostic classifiers separating HC, SCZ, and MDD patients based on resting-state EEG recordings, (2) constructing a novel, electrophysiological measure of brain aging estimate in SMI, that is, Electrophysiological Age Gap Estimation (EphysAGE), and (3) investigating the impact of EphysAGE on (differential) diagnostic separability. There are shared signatures between healthy aging and SMI patterns such as the decreased alpha band power as well as distinct differences in the delta and theta waves. Thus, we hypothesize a complex interplay between age-related changes and the neural signatures of SCZ and MDD to be extractable from EEG recordings by using advanced mathematical modeling, which might otherwise be obscured, or masked if lower-level univariate statistics would be employed.

Methods and Materials

Study Participants

The data were collected in the Department of Psychiatry and Psychotherapy of the LMU University Hospital, LMU Munich, between 2012 and 2018. A total of 735 participants were included, comprising 250 individuals, who met the diagnostic criteria for SCZ and 240 individuals for MDD according to ICD-10[63] as well as 245 HC individuals (Supplementary table 1). The EEG recordings were performed in the clinical setting either as a routine diagnostic measure or as a part of electrophysiological studies within separate research protocols (Supplementary Methods, Supplementary table 2). All participants that are included in the studies provided written consent prior to single-site study inclusion. The study was approved by the local ethics committee of LMU (Reference Number: 22-0771). The study adhered to the ethical principles outlined by the pertinent national and institutional boards for human experimentation and followed the 2008 revised version of the Declaration of Helsinki.[64]

Electrophysiological Data Acquisition

Electroencephalographic Recordings EEG recordings of each participant were acquired in eyes-closed condition for 10 min using an electrode cap with 19 electrodes, and an additional electrooculogram channel to record eye movements placed according to the 10–20 system.[65] A Neuroscan Synamps apparatus was used for the recordings in the Department of Psychiatry and Psychotherapy, University Hospital of the Ludwig-Maximilians-University. The sampling frequency at recording was 1000 Hz, which was downsampled to 250 Hz before further analysis steps. Electrode skin impedance was always less than 5 kΩ. All sensor electrodes were referenced to the channel Cz.

Data Preprocessing The software BrainVision Analyzer (BrainVision Analyzer, Version 2.2.2, Brain Products GmbH) was used for bandpass filtering between 1 and 70 Hz, and notch filtering for 50 Hz line noise of the recordings, and all sensor electrodes were re-referenced to the average reference. The absolute values were calculated for each recording. The technicality and muscle artifacts as well as eye movement artifacts were visually inspected and cleared from the data by the trained psychiatrists and psychologists with expertise in EEG in our clinic. At least 60 s of artifact-free data segments were selected from every recording to enter the analysis pipeline.

Feature Extraction Data analysis was performed with Brainstorm version 3.220503[66] (freely available at http://neuroimage.usc.edu/brainstorm). We calculated the power spectrum density to produce frequency domain features.[67] To better capture the nonstationarities in the oscillatory activity, Welch transformation was applied between 1 and 70 Hz with a step of 1 Hz using a window of one second with 50% overlap using fast Fourier transform defaults for every channel.[68] This procedure yielded 1330 power spectrum density features for each participant. Furthermore, we computed NxN Pearson's correlation coefficients between all available EEG channels amounting to 171 connectivity features per individual after eliminating the auto-correlations and doubled measurements.[69] A total of 1501 features entered the ML pipeline.

ML Analysis

The open-source ML platform NeuroMiner (version 1.1; http://proniapredictors.eu/neurominer/index.html) was used to train support vector machine (SVM) models with a linear kernel on both EEG modalities combined through stacking (power spectrum density, connectivity). To enhance the models' generalizability and prevent overfitting, we adopted a pooled nested cross-validation strategy with 10-fold and 10 permutations on both the CV1 and CV2 levels. This strategy completely insulated the model training from the model testing process by performing hyperparameter optimization at the CV1 level, while validating model performance exclusively at the CV2 level.[70–73] First, we built two SVM classification models to distinguish SCZ patients from HC individuals (SCZ classification model) and MDD patients from HC individuals (MDD classification model). Second, we built an SVM differential diagnostic model separating SCZ from MDD patients. Third, we compared our diagnostic and differential diagnostic performances to multigroup models that were trained in two different repeated nested cross-validation schemes (One-vs-all and one-vs-one, Supplementary Material). In the preprocessing pipeline of all three classification models, beta coefficients of linear associations between age and power spectrum density or connectivity features were computed in the CV1 training data of the HC group using partial correlation analysis. These coefficients were subsequently employed to correct the respective data of both patient and HC samples in the CV1 training, CV1 testing, and CV2 validation partitions (Supplementary Material).[74,75] Third, we used support vector regression (SVR) to train and cross-validate an EphysAGE model, that is, a normative age-prediction model in the HC population (Supplementary Material). When training the model, we used explained variance (R^2) as the optimization criterion. EphysAGE was then calculated as the difference between the predicted age from the EphysAGE model and the chronological age. The EphysAGE model was then applied to the SCZ and MDD populations to estimate their electrophysiological age.

Medication Effects To decide whether to correct the EEG features for medication effects, the chlorpromazine equivalence (CPZ) dosage for antipsychotic medications[76–78] and fluoxetine (FLUOX) dosage equivalence for antidepressant medication[79] were calculated. We investigated associations between medication dose and the EphysAGE scores extracted from the regression model by means of Pearson's linear correlation coefficient.[80] Additionally, we conducted two supplementary SVM classification analyses classifying the medicated and nonmedicated patients separately for SCZ and MDD.

Classification Models Balanced accuracy (BAC), defined as the mean of sensitivity and specificity, was used as the optimization criterion for the three SVM classification models. We calculated the rank-transformed decision scores[81] produced by the three classifiers as the transformed distance between the position of the given individual in the linear kernel space and the optimally separating hyperplane. Rank transformation of decision scores was performed to enhance the interpretability and facilitate between-classifier comparisons. Specifically, a percentile rank-transformed score of 80% indicates that the subject's score exceeds that of 79.9% of the population

under study, placing the subject in the top 20% of the distribution. Hence, higher positive rank-transformed decision scores reflect increased likeness of the positive label and vice versa for the negative label. We also assessed residual age effects on classifier performance across five age bins (16–25, 26–35, 36–45, 46–55, and 56–65 years). The significance of the association between predicted labels and group membership of the models in each age bin was evaluated using the χ^2 test.[80] Furthermore, to assess model specificity a cross-diagnostic model application approach was implemented by applying the trained SCZ Model to MDD patients' data and vice versa. Cross-over model performance was calculated as the percentage of individuals from the other patient group being case labeled. Finally, we used Kruskal–Wallis' H Test[82] and Dunn–Sidak's post hoc comparison test[83] (HC as reference group) to evaluate rank-transformed decision scores for group-level differences. Statistical significance was determined at $\alpha = .05$.

EphysAGE Model Using explained variance (R^2) as the optimization criterion for the SVM regression model, we first predicted age in HC and then applied this normative model to the data of patient groups. Regression models often exhibit increased prediction errors toward the extremes of the label distribution. This phenomenon can be corrected by (1) calculating the slope between labels and prediction errors using a reference dataset and (2) applying the correction parameters on the predictions of a target sample. Therefore, this post hoc tail offset correction is customary for BrainAGE analyses.[84] The correction parameters were calculated in our HC sample, and then used to adjust the SCZ and MDD patients' age predictions. Group differences in EphysAGE were assessed using the nonparametric Kruskal–Wallis H test, with Dunn–Sidak's post hoc multiple comparison tests for individual group comparisons,[82,83] since EphysAGE scores were not normally distributed. Finally, we explored the additional value of EphysAge in our diagnostic and differential diagnostic classification models by implementing EphysAGE as an additional modality and feature to our models (Supplementary Material).

Model Significance and Visualization The significance of the SVM models was assessed by comparing their performances (BAC) against a null distribution of 1000 models trained on the same dataset with random permutations of the labels.[71,85] In each permutation, the models were retrained within the cross-validation framework using the respective label subsets corresponding to the observed-label analyses. During each permutation, predictions were gathered from randomized models to create a permuted ensemble prediction for each CV2 subject. Consequently, a null distribution of out-of-training classification performance was established for the prediction models. To assess the significance of the observed out-of-training BAC, we computed the number of instances where the permuted out-of-training BAC equaled or exceeded the observed BAC. Model significance was determined at a P value threshold of $<.05$.

Models were visualized by back-projecting model weights to the original data space. Pattern element stability and significance of the SVM model feature weights were estimated using the measures of cross-validation ratio (CVR) and sign-based consistency, respectively.[86,87] CVR represents the sum of the median weights from all CV1 folds, divided by the standard deviation. It is an indicator of how stable features contribute to the predictive pattern. Sign-based consistency assesses how consistently a variable was either positively or negatively weighted across the CV partitions. This method allows us to compute a P value for each feature in the dataset to determine whether this sign-based consistency is above the chance level. Features with a CVR $\geq |2|$ and a false discovery rate corrected P value $<.05$ were defined as reliable and significant predictors. Specifically, the median of the CVR for each frequency interval: delta (1–3 Hz), theta (4–7 Hz), alpha (8–11 Hz), beta (12–29 Hz), low-gamma (30–49 Hz), and high-gamma (50–70 Hz) was calculated for those features, which were deemed significant by sign-based consistency mapping. Furthermore, the association between chronological age and power spectrum density was investigated with Pearson's correlation method (Supplementary Material). The CVR values of correlation-based EEG features were further analyzed using an undirected graph-theoretical approach.[88] Subsequently, their contribution to the models' predictive patterns was assessed via eigenvector centrality which is a measure of the influence of a node, for example, channels, in a network[88] (Supplementary Material).

Results

Sample Characteristics

SCZ patients (mean[SD], 36.5[11.4]) were significantly younger and more predominantly male (93, 62.8% male) compared to MDD patients (44.3[14.4], $P = 1.12 \times 10^{-8}$, 145 (39.4% male) and HC individuals (47.0[4.5], $P = 9.67 \times 10^{-16}$, 121 (51.14% male). 146 out of 240 (60.8%) MDD patients and 90 out of 250 (36.0%) SCZ patients were unmedicated (Supplementary table 1).

Medication Effects

The EphysAGE scores of medicated patients were not correlated with CPZ dosage for SCZ and FLUOX dosage for the MDD group ($\rho_{CPZ} = -0.05$, $P = .60$ and $\rho_{FLUOX} = -0.06$, $P = .57$). Additionally, the two models distinguishing medicated from nonmedicated patients with the SCZ or MDD groups did show predictive performances close to chance levels (SCZ: BAC = 55%; MDD: BAC = 52%; Supplementary Material). Therefore,

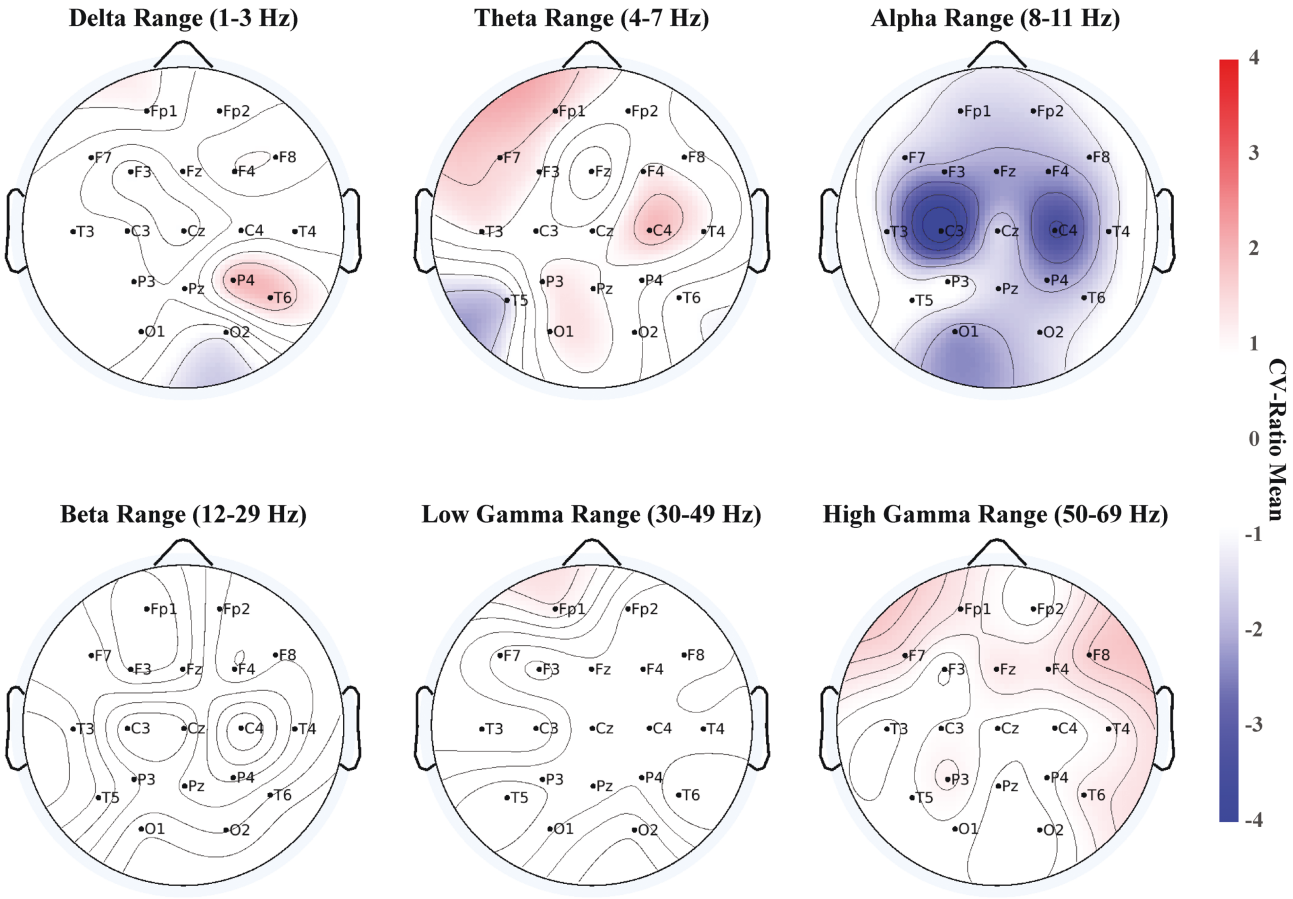

Fig. 1. Topographical plots of overall mean of CVR in classification models—SCZ Model. The topographical representations with channel locations and names of CV ratio overall mean values in the frequency power domain for three classification models are illustrated. Frequency ranges: delta: 1–3 Hz, theta: 3–7 Hz, alpha: 8–11 Hz, beta: 12–19 Hz, low-gamma: 20–49 Hz, high-gamma: 50–70 Hz. SCZ Model: decreased alpha frequency power was predictive of SCZ likeness.

we did not correct for medication effects in the differential diagnostic or age prediction analyses.

Classification Models

The SCZ classification model correctly identified 179 out of 250 SCZ (sensitivity, SEN = 71.6%) and 181 out of 245 HC individuals (specificity, SPEC = 73.9%), yielding a cross-validated BAC of 72.7%, a positive predictive value (PPV) of 73.7% and a negative predictive value (NPV) of 71.8% ($P_{1000} < .001$). In the SCZ model, global alpha oscillation power decrease was predictive of SCZ (figure 1). Centrality values derived from the undirected graph network peaked between the C4 and F7 followed by Fp1 electrodes.

The MDD classification model correctly identified 163 out of 240 MDD (SEN = 67.9%) and 162 out of 245 HC individuals (SPEC = 66.1%), with a cross-validated BAC of 67%, a PPV of 66.3%, and an NPV of 67.8% ($P_{1000} < .001$). Higher global delta frequency power was predictive of MDD status, while frontal theta frequency power contributed to HC classification (figure 2). The MDD Model showed the highest centrality in central and frontal regions based on the undirected graph.

The classification performance of the SCZ and MDD Models peaked in the second youngest (26–35 years) age bin (SCZ: SEN = 85.7%, $\chi^2 = 31.2$, $P = 2.35e^{-6}$; MDD: SEN = 80.0%, $\chi^2 = 23.8$, $P = 1.06e^{-6}$). Both classification models performed worst in the oldest age group (56–65 years, SCZ: SEN = 42.9%, $\chi^2 = 9.7$, $P = .002$; MDD: SEN = 61.9%, $\chi^2 = 13.7$, $P = 2.13e^{-4}$; table 1).

The differential diagnostic model (SCZ vs MDD) correctly detected 179 of 250 SCZ (71.6%) and 130 of 240 MDD patients (54.2%), resulting in a BAC of 62.88%, a PPV of 61.94%, and a NPV of 64.68% ($P_{1000} < .001$). Overall delta frequency power was indicative of SCZ class membership while high-gamma oscillations predicted MDD status (Supplementary figure 3). The highest centrality was observed for the P3, C4, and Fp1 electrodes.

The SCZ Model case labeled, that is, labeled as SCZ, 55.0% of the MDD patients. Specifically, SCZ patients had the highest rank-transformed decision scores, that is, the likelihood to be classified as SCZ (median[interquartile range (IQR)], 70.5[IQR:38.2]) followed by MDD patients

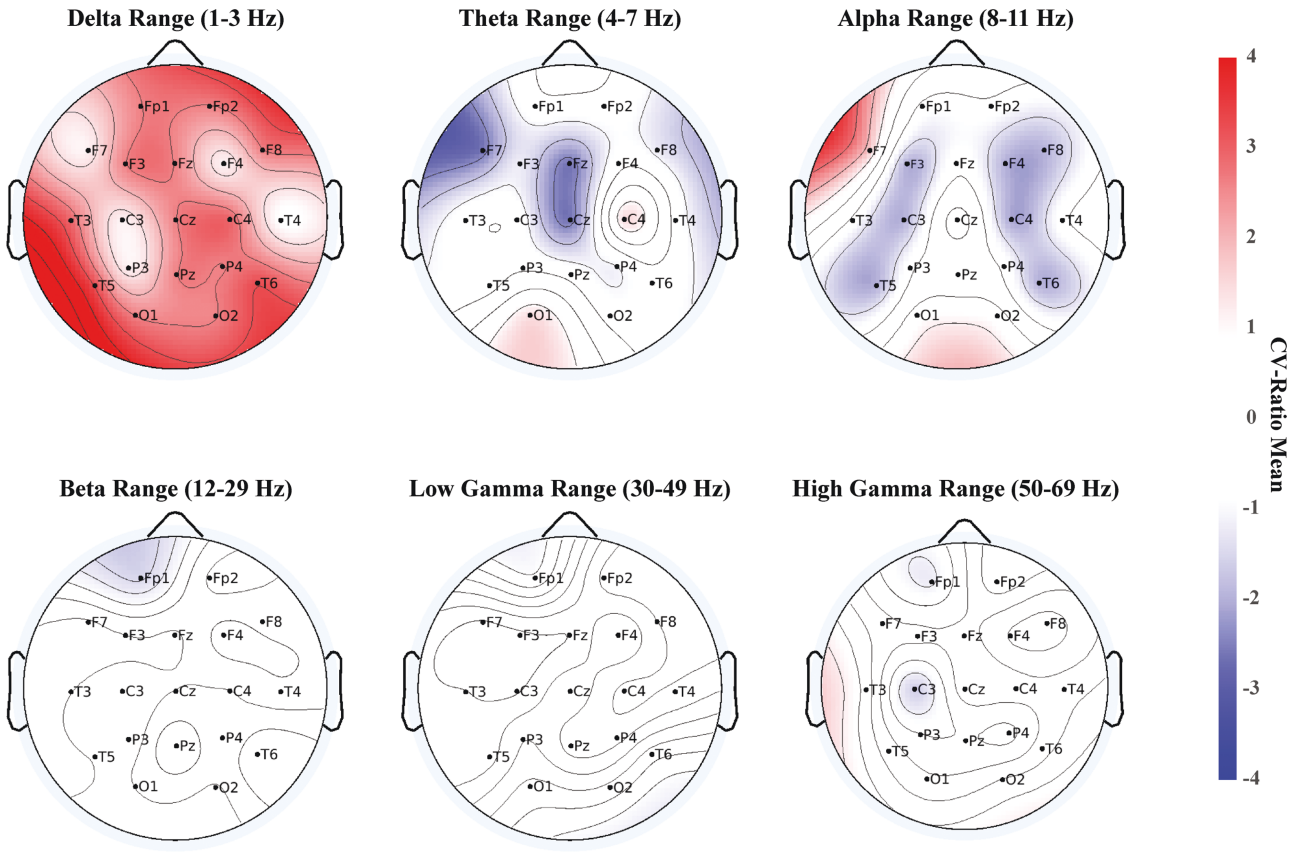

Fig. 2. Topographical plots of overall mean of CVR in classification models—MDD Model. Overall increased delta frequency power decreased central and left temporal theta power as well as decreased central alpha power along with decreased left temporal alpha power were predictive of MDD likeness.

(56.5[IQR:40.8]) and HC individuals (30.8[IQR:38.0]; $\chi^2 = 151.6$, df = 2, $P = 1.2e\text{-}33$). The MDD Model case labeled, that is, labeled as MDD, 82.10% of the SCZ individuals (figure 3). Notably, SCZ patients yielded higher rank-transformed decision scores (78.7[IQR:29.2]), that is, a higher likelihood to be classified as MDD, compared to MDD patients (65.6[IQR:42.0]), and HC individuals (34.9[IQR:43.5], $\chi^2 = 160.0$, df = 2, $P = 1.8e\text{-}35$).

The multigroup classifier trained in an all-vs-one repeated nested cross-validation scheme which distinguishes one group from the two other groups, performed at chance level (Supplementary figures 1 and 2). In contrast, the multigroup classifier trained in a one-vs-one cross-validation scheme performed at a similar level to the original binary classifiers (Supplementary figures 2 and 3).

Furthermore, the SVM classifiers distinguishing medicated from nonmedicated patients did not identify medicated individuals above chance level after permutation testing ($P > .05$), which supported our initial approach not to correct our models for medication effects (Supplementary Material). Additionally, the fluoxetine and CPZs were not significantly correlated with EphysAGE in medicated MDD ($P = -.06$, $P = .57$) or SCZ patients ($P = -.05$, $P = .60$).

EphysAGE Model

The EphysAGE model predicted age in HC individuals with an explained variance of 46% (MAE = 8.7 years, T = 14.31, $P_{1000} < .001$). Central higher delta frequency as well as occipital and temporal lower high-gamma frequency power predicted higher age (Supplementary figure 4). Centrality in the EphysAGE model peaked at T5, T4, and P3 electrode regions (Supplementary table 5).

When applied to the two patient groups, the Kruskal–Wallis H test revealed significant differences between HC, MDD, and SCZ individuals ($\chi^2 = 6.46$, $P = .04$). Dunn–Sidak's post hoc multiple comparison test showed no significant difference between patient groups and HC regarding their EphysAGE (SCZ vs HC, $P = .80$; MDD vs HC, $P = .17$). However, the EphysAGE of SCZ patients was significantly higher than of MDD patients (SCZ vs MDD, $P = .04$).

Interaction Between EphysAGE and (Differential) Classification Performance

The EphysAGE scores of HC individuals and MDD patients were positively correlated with their rank-transformed SCZ scores indicating that their SCZ

Table 1. Performance Metrics of the EEG-based Classification Models

	SENS (%) (95% CI)	SPEC (%) (95% CI)	BAC (%) (95% CI)	PPV (%) (95% CI)	NPV (%) (95% CI)	AUC (95% CI)	χ^2	*P*
SCZ Classification Model								
Overall (*N* = 495)	71.60 (67.91–73.32)	73.88 (70.07–76.96)	72.73 (69.71–74.42)	73.66 (70.36–75.92)	71.83 (68.76–73.30)	0.73 (0.68–0.77)	102.4	**4.54E-10**
16–25 years (*N* = 65)	84.78 (79.01–86.95)	52.63 (42.71–64.29)	68.71 (62.36–74.13)	81.25 (77.50–84.98)	58.82 (48.66–64.35)	0.69 (0.55–0.82)	9.75	**.002**
26–35 years (*N* = 127)	85.71 (80.46–88.25)	62.00 (57.16–68.21)	73.86 (70.01–76.99)	77.65 (74.94–80.42)	73.81 (66.82–77.73)	0.74 (0.65–0.82)	31.18	**2.35E + 06**
36–45 years (*N* = 118)	69.62 (64.23–74.20)	61.54 (57.37–73.94)	65.58 (62.53–72.33)	78.57 (76.32–84.38)	50.00 (46.13–56.50)	0.66 (0.55–0.76)	10.5	**.001**
46–55 years (*N* = 73)	40.63 (28.76–47.88)	73.17 (70.60–79.21)	56.90 (51.36–61.50)	54.17 (47.55–60.95)	61.22 (57.14–64.71)	0.57 (0.44–0.70)	1.55	.21
56–65 years (*N* = 106)	42.86 (28.31–63.23)	89.13 (78.99–91.40)	65.99 (57.36–73.64)	37.50 (21.78–42.82)	91.11 (88.76–93.64)	0.66 (0.50–0.82)	9.7	**.002**
MDD Classification Model								
Overall (*N* = 485)	67.92 (63.48–70.72)	66.12 (63.92–69.55)	67.02 (64.60–69.24)	66.26 (64.13–68.67)	67.78 (64.82–70.07)	0.67 (0.62–0.72)	56.2	**6.54E-14**
16–25 years (*N* = 43)	58.33 (50.20–71.31)	47.37 (38.76–56.74)	52.85 (46.53–61.97)	58.33 (52.82–66.07)	47.37 (40.05–58.33)	0.53 (0.35–0.70)	0.14	.71
26–35 years (*N* = 95)	80.00 (69.08–84.33)	70.00 (64.64–76.59)	75.00 (68.77–78.54)	70.59 (65.32–75.01)	79.55 (71.28–83.10)	0.75 (0.65–0.85)	23.81	**1.06E-06**
36–45 years (*N* = 103)	68.75 (61.62–73.39)	66.67 (58.60–71.09)	67.71 (62.50–70.85)	77.19 (72.00–79.82)	56.52 (49.42–60.46)	0.68 (0.57–0.78)	12.3	**4.53E-04**
46–55 years (*N* = 88)	68.09 (58.20–75.21)	56.10 (52.47–67.67)	62.09 (57.51–69.28)	64.00 (60.38–71.04)	60.53 (54.27–68.21)	0.62 (0.50–0.74)	5.22	**.02**
56–65 years (*N* = 136)	61.92 (56.02–67.95)	71.74 (68.45–76.34)	66.55 (64.03–70.30)	50.94 (48.01–55.54)	79.52 (77.48–82.38)	0.67 (0.56–0.77)	13.71	**2.13E-04**
Differential Diagnostic Model (SCZ vs MDD)								
Overall (*N* = 490)	71.6 (69.30–74.41)	54.17 (51.74–57.73)	62.88 (61.22–65.37)	61.94 (60.48–64.16)	64.68 (62.60–67.64)	0.63 (0.58–0.68)	33.6	**6.76E-09**
16–25 years (*N* = 70)	97.83 (94.32–100)	0 (–2.03–2.87)	48.91 (47.35–50.35)	65.22 (64.49–65.88)	0	0.49 (0.34–0.63)	0.53	.47
26–35 years (*N* = 122)	97.40 (92.04–99.05)	17.78 (12.20–24.13)	57.59 (53.61–60.09)	66.96 (64.95–68.35)	80.00 (54.87–87.02)	0.58 (0.47–0.68)	8.7	**.003**
36–45 years (*N* = 143)	70.89 (66.77–77.40)	34.38 (30.58–44.75)	52.63 (51.03–58.72)	57.14 (55.96–61.68)	48.89 (46.34–58.09)	0.53 (0.43–0.62)	0.45	.5
46–55 years (*N* = 79)	9.38 (6.50–19.58)	87.23 (81.03–92.20)	48.30 (45.50–54.16)	33.33 (23.40–56.48)	58.57 (56.99–61.81)	0.48 (0.35–0.61)	0.22	.64
56–65 years (*N* = 58)	0 (–4.16–6.98)	97.73 (92.15–100)	48.86 (45.15–52.36)	0	75.44 (74.01–76.77)	0.49 (0.31–0.66)	0.32	.57

Note: The performance of three classification models (SCZ, MDD, and Differential Diagnostic Models) are represented in five different 10-year apart age bins (16–25, 26–35, 36–45, 46–55, 56–65) along with their overall performances. Highest sensitivity was found in the youngest age bin for SCZ and Differential Diagnostic Model and in the 36–45 years age bin for MDD Model. In all three models, the highest BAC was achieved in the 26–36 years of age group. SEN, sensitivity; SPEC, Specificity; BAC, balanced accuracy; NPV, negative predictive value; PPV, positive predictive value; *P* value threshold = .05.

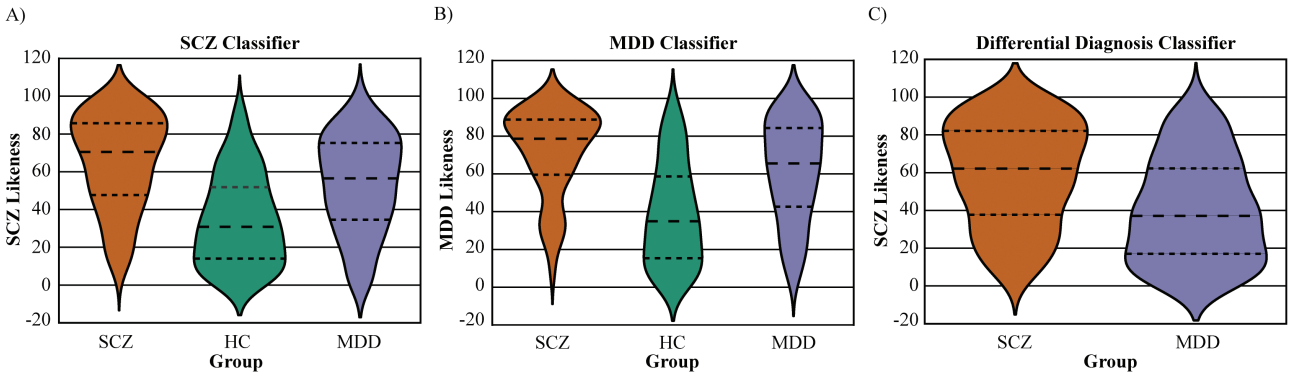

Fig. 3. Model specificity assessment with cross-diagnostic application. Difference of the mean decision scores in different groups for all classification models. (A) In SCZ Model, all three groups' decision scores are different from each other, and the highest decision scores are in the patients with SCZ followed by patients with MDD then the HC individuals. (B) In MDD model, again the three groups are different from each other in terms of their decision scores and the gradual change is in the same ranking as the SCZ Model. (C) In the differential diagnostic model, the mean decision scores in patients with SCZ are significantly higher than in MDD patients. All three models indicate a gradual change in the disease signature between SCZ and MDD.

classification likelihood increased with higher EphysAGE ($\rho_{HC} = 0.23$, $P = 3.42 \times 10^{-4}$; $\rho_{MDD} = 0.17$, $P = .01$). No such correlation was found for SCZ individuals ($\rho_{SCZ} = -0.08$, $P = .21$, figure 4). Also, no significant correlations were detected between EphysAGE and rank-transformed MDD decision scores. In the differential diagnostic model, a significant correlation between EphysAGE and rank-transformed decision scores was observed found: In the SCZ group, SCZ likeness decreased with higher EphysAGE ($\rho_{SCZ} = -0.15$, $P = .02$) while it increased in the MDD sample ($\rho_{MDD} = 0.14$, $P = .03$). Finally, the models that contained EphysAGE as an additional feature performed at similar levels with the original binary classifiers. The EphysAGE was a predictive feature only when added to the differential diagnostic classifier (CVR = −2.15, Supplementary Material).

Discussion

We used resting-state EEG and supervised ML in a large, naturalistic single-site cohort to quantify aberrant brain aging processes and assess their impact on diagnostic separability. First, we developed three EEG-based classification models that robustly discriminated SCZ and MDD patients from HC individuals, and, to a lesser degree, SCZ from MDD patients. Second, we developed an EEG-based normative age prediction model, revealing that SCZ patients had higher EphysAGE than MDD patients. Third, we showed that higher electrophysiological brain aging, that is, higher EphysAGE scores, negatively impacted the identification of MDD and HC in the SCZ classification model and the identification of both MDD and SCZ patients in the differential diagnostic model (SCZ vs MDD).

Exploration of the SCZ model revealed alpha power decrease in frontal, central, and left occipital brain regions as the most predictive features for SCZ, which is in line with previous findings.[89–91] In these previous studies, reduced alpha power and decreased alpha coherence were correlated with negative symptoms, impairments in visual perception, and poorer cognitive performance in task-dependent conditions,[90,92–94] thereby linking these changes to early disrupted perceptual processing in SCZ. In resting-state conditions, alpha rhythm voltage has been linked to a decrease in cortical excitability and attention.[95]. Moreover, a link has been suggested between alpha rhythm amplitude, cortical excitability, and cholinergic pathways in the forebrain.[95,96] Thus, this pattern could represent an electrophysiological signature of SCZ, linking widespread alpha power decrease as well as dysfunctional cholinergic transmission and glutamatergic hypofunction to characteristic clinical impairments.[97,98] Moreover, these processes are speculated as being facilitated by reduced kainate receptor density in both psychotic and affective disorders.[99]

The MDD classification model rested on overall delta power increase and alpha power decrease to separate study participants. While these findings further support the role of disrupted alpha rhythm in MDD, they do not replicate the previously reported frontal alpha asymmetry in MDD[100,101] which was in itself rebutted in a recently published meta-analysis.[18] Rather, a central bilateral alpha power decrease was observed in our model derived from our naturalistic sample.

Moreover, we observed classification asymmetry in our cross-diagnostic analysis, with the SCZ model case-labeling MDD individuals in 55.8% of cases, while the case-labeling of SCZ patients occurred at a much higher rate (82.1%) in the MDD Model. Hence, the SCZ Model might have captured an electrophysiological signature that is more specific to SCZ pathophysiology, while the MDD Model represents a more general SMI signature, which distinguishes MDD and SCZ as SMIs in general from HC individuals. This interpretation may be seen

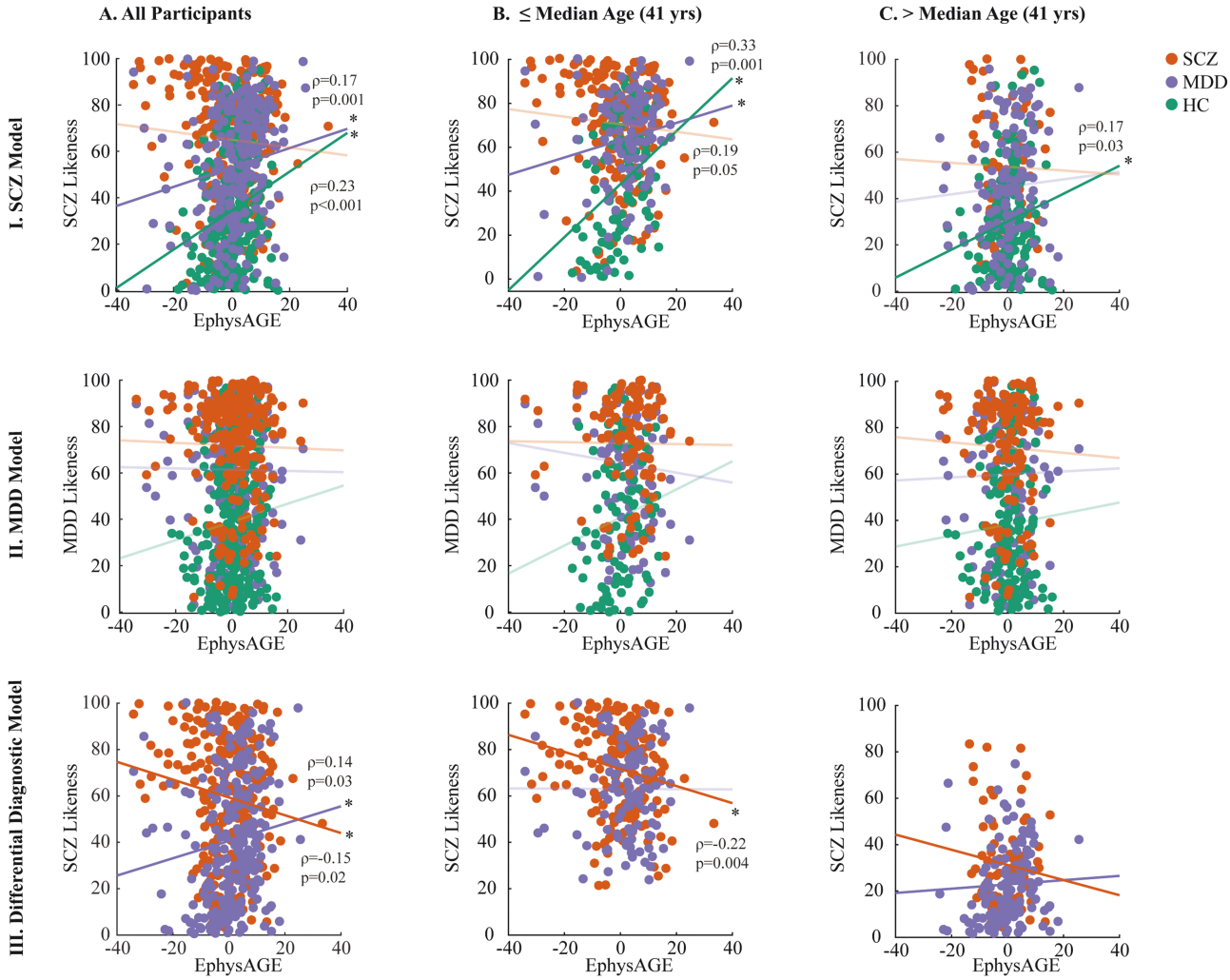

Fig. 4. EphysAGE correlations with SMI likeness. Correlations between rank-transformed decision scores derived from the classification models and EphysAGE are investigated in younger and older age groups. In the SCZ Model, (I) EphysAGE of MDD and HC groups are positively correlated with SCZ-likeness, that is, when EphysAGE is higher in these two groups, they are more likely to be misclassified as SCZ. These correlations are more prominent in the younger age groups. (II) In the MDD Model, there is no significant correlation between the group assignment and EphysAGE in any age group. In the differential diagnostic model, (III) Higher EphysAGE in the SCZ group is correlated with misclassification as MDD and higher EphysAGE in the MDD group is correlated with misclassification as SCZ in the all participant group. The correlation between the SCZ group's misclassification with higher EphysAGE consists in the young age group.

as consistent with the triadic system of mental illness[102] where depressive symptoms constitute a transnosological external circle common to many different psychiatric disorders which envelopes an inner circle that contains SCZ characterized by more specific, or endogenous symptoms.[48,103] An alternative explanation of our findings could align with the hypothesis that a subgroup of MDD is more closely aligned with SCZ in terms of a common functional brain substrate, while the rest of the MDD population exhibits a mixed brain pathology not related to SCZ.[75] The one-vs-all multigroup classifiers performed significantly much lower than the original binary classification models. This could be attributed to the greater diversity within the "all" groups, which included combinations of HC and MDD, HC and SCZ, or MDD and SCZ, depending on the setup. On the other hand, the one-vs-one multigroup classification approach involves pairwise classifications between two distinct groups. This makes them comparable to the binary models which might, in turn, explain why they exhibited similar performance levels.

In the EphysAGE model, the spectral features most strongly predictive of older age included increased power in overall delta and frontal and temporal theta frequency intervals. Although a slow-wave power change in healthy aging was consistently reported in the literature,[10,61,62,104,105] there is still much controversy regarding the direction of this power change. While several studies found a decrease in slow waves in EEG and magnetoencephalography with increased age,[62,106,107] other studies reported an increase

in delta and theta power correlating with older age in resting-state recordings.[10] Notably, the alpha power which was found to decrease in healthy aging in previous studies,[10,62,108,109] was not a significant predictor of age in our model. Consistent with previous studies, we found frontotemporal and central electrodes to be predictive of higher age.[110] Similar to the MRI-based BrainAGE measure,[111,112] progressive and regressive neurobiological processes such as the glucocorticoid cascading hypothesis, which suggests a feed-forward mechanism between the psychosocial daily stressors and both aging and psychotic experiences[113,114] might also underlie these electrophysiological patterns. Therefore, pathological accelerated aging is not only detectable in structural brain patterns but can in fact also be observed in changes in neural activity as measured by EphysAGE.

Furthermore, the correlation between EphysAGE and classification likelihood offers additional insight into the link between accelerated aging, disease-related electrophysiological aberrations, and diagnostic separability. The positive correlation between EphysAGE in MDD and HC individuals and the likelihood of being case labeled as SCZ could be reflective of a pathophysiological proximity between MDD patients with accelerated brain aging and SCZ patients.[48,115,116] Moreover, the difference in EphysAGE between individuals with MDD and SCZ could further substantiate this argument. For SCZ individuals, the inverse association between EphysAGE and the likelihood of being correctly classified in the differential diagnostic model might indicate that the electrophysiological disease signature of SCZ becomes "diluted" as the disease progresses and EphysAGE increases. This could be speculatively interpreted as a "multilayered aging" process where the electrophysiological disease signatures become increasingly blurred and less specific, therefore being increasingly masked by diffuse aging and degeneration patterns[43,48] caused, for example, by the somatic sequelae of poor lifestyles, and/or social deprivation effects. Further support for this hypothesis is derived from our finding that with increasing age, the sensitivity of the SCZ and MDD classification models decreases, while their specificity increases. Hence, in contrast to BrainAGE findings, the models become less accurate in identifying the disorders with higher age in EEG recordings, which, again, could be attributed to an increased "dilution" of discriminative neural signals. Indeed, previous studies found that the structural brain signature of SCZ becomes more distributed and diffuse as the disease progresses, making it less distinct.[117] Therefore, BrainAGE, a structural signature, differs fundamentally from EphysAGE, an electrophysiological signature, as BrainAGE appears more pronounced and predictive as age increases.[118] EphysAGE, on the other hand, becomes more diffuse and less predictive. This could be attributed to counteracting processes between physiological aging and disease effects of SCZ and MDD, such as inverse directionality in high-gamma oscillations power and absence or presence of theta and delta frequency powers patterns. Therefore, younger patients in earlier disease stages would carry more specific electrophysiological disease signals, which are not yet overly influenced by physiological and pathological aging processes, making EEG-based biomarkers most well-suited for early recognition and intervention purposes. Furthermore, our results suggest that EphysAGE may be most effective when used in conjunction with other features rather than as the sole predictor, especially in the differential diagnosis.

Beyond these findings, several limitations should be noted. First, the lack of a deeper clinical phenotyping of our sample did not allow for a more in-depth investigation of possible crosslinks and interactions between EphysAGE and other markers of disease progression. Thus, more deeply phenotyped samples would enable more fine-grained investigations into how prediction performance, EphysAGE, and feature importances may be influenced by the age of onset and the duration of the disease, the outcome of the treatment as well as the effect of the severity of different symptoms. Through these analyses, researchers could gain a more comprehensive understanding of how different disease facets impact on neural activity. Such investigations hold the potential to unveil novel biomarkers, enhance predictive models, and ultimately advance diagnostic and treatment approaches for individuals impacted by SMI. Furthermore, the substantial chronological age gap between SCZ and HC individuals might have negatively impacted the EphysAGE model since the accelerated brain aging in SCZ individuals might have brought them "biologically closer" to the already older HC population, even though the classification models were corrected for age in the classification models. Moreover, only the eyes-open condition of the resting-state EEG recordings was included in the current work (Supplementary Material). Lastly, external validation approaches should be employed to assess the generalizability of our models in independent samples.

Conclusion

In summary, our findings indicate that ML techniques applied to routine EEG data can generate diagnostic models. These models should be translated into clinical practice in early disease stages where the impact of physiological and pathological aging processes is still limited, and the electrophysiological brain signatures provide higher discriminative power. A timely and targeted application of such EEG-based models could lead to noninvasive, cost-effective biomarkers of neural activity in severe mental disorders.

Supplementary Material

Supplementary material is available at https://academic.oup.com/schizophreniabulletin.

Acknowledgments

The funding organizations were not involved in the design and conduct of the study; the collection, management, analysis, and interpretation of the data; the preparation, review, or approval of the manuscript; and the decision to submit the manuscript for publication.

Author Contributions

ES, OP, and DK had full access to all the data in the study and take responsibility for the integrity of the data and the accuracy of the data analysis. Acquisition, analysis, or interpretation of data: ES, DP, NK, AK, DK, OP; drafting of the manuscript: ES, DP; critical revision of the manuscript for important intellectual content: ES, DP, AK, NK, DK, OP, KS, PF; statistical analysis: ES; administrative, technical, or material support: NK, DK, OP, KS, PF; supervision: DP, NK, OP, KS, PF.

Conflict of Interest Statement

NK owns issued patent US20160192889A1 ("Adaptive pattern recognition for psychosis risk modeling"). As a member of Spring Health's Scientific Advisory Board, NK has advised that company on the development of tools to predict treatment outcomes for depression and psychosis. He has no equity and has received no financial compensation from this company. PF received research support/honoraria for lectures or advisory activities from Boehringer-Ingelheim, Janssen, Lundbeck, Otsuka, Recordati, and Richter. These affiliations did not influence the writing of this manuscript. No other disclosures are reported.

Funding

This work was supported by the "Else-Kröner-Fresenius-Stiftung" through the Clinician Scientist Program "EKFS-Translational Psychiatry" (DP); National Institutes of Health (U01MH124639-01; ProNET), the Wellcome Trust, the German Innovation Fund (CARE project), the German Federal Ministry of Education and Research (COMMITMENT and BEST projects), as well as ERA PerMed (IMPLEMENT project) (NK); German Federal Ministry of Education and Research (COMMITMENT 01ZX1904E to AK); PF has received and is currently receiving grants from several national and international foundations and institutions, for example, from the "German Science Foundation," the "German Ministry of Science," and the "German Ministry of Health."

References

1. Berger H. Über das Elektrenkephalogramm des Menschen. *Arch Für Psychiatr Nervenkrankh*. 1929;87(1):527–570. doi:10.1007/BF01797193
2. Millett D. Hans Berger: from psychic energy to the EEG. *Perspect Biol Med.* 2001;44(4):522–542. doi:10.1353/pbm.2001.0070
3. Fingelkurts AA, Fingelkurts AA. Altered structure of dynamic electroencephalogram oscillatory pattern in major depression. *Biol Psychiatry* 2015;77(12):1050–1060. doi:10.1016/j.biopsych.2014.12.011
4. Rockstroh BS, Wienbruch C, Ray WJ, Elbert T. Abnormal oscillatory brain dynamics in schizophrenia: a sign of deviant communication in neural network? *BMC Psychiatry* 2007;7:44. doi:10.1186/1471-244X-7-44
5. Newson JJ, Thiagarajan TC. EEG frequency bands in psychiatric disorders: a review of resting state studies. *Front Hum Neurosci.* 2019;12:521. doi:10.3389/fnhum.2018.00521
6. Harmony T. The functional significance of delta oscillations in cognitive processing. *Front Integr Neurosci.* 2013;7:83. https://www.frontiersin.org/articles/10.3389/fnint.2013.00083. Accessed December 10, 2023.
7. Amzica F, Steriade M. Electrophysiological correlates of sleep delta waves1. *Electroencephalogr Clin Neurophysiol.* 1998;107(2):69–83. doi:10.1016/S0013-4694(98)00051-0
8. Hagihira S. Brain mechanisms during course of anesthesia: what we know from EEG changes during induction and recovery. *Front Syst Neurosci.* 2017;11:39. doi:10.3389/fnsys.2017.00039
9. Sauseng P, Griesmayr B, Freunberger R, Klimesch W. Control mechanisms in working memory: a possible function of EEG theta oscillations. *Neurosci Biobehav Rev.* 2010;34(7):1015–1022. doi:10.1016/j.neubiorev.2009.12.006
10. Klimesch W. EEG alpha and theta oscillations reflect cognitive and memory performance: a review and analysis. *Brain Res Brain Res Rev.* 1999;29(2-3):169–195. doi:10.1016/S0165-0173(98)00056-3
11. Hughes JR, John ER. Conventional and quantitative electroencephalography in psychiatry. *J Neuropsychiatry Clin Neurosci.* 1999;11(2):190–208. doi:10.1176/jnp.11.2.190
12. Gattaz WF, Mayer S, Ziegler P, Platz M, Gasser T. Hypofrontality on topographic EEG in schizophrenia: correlations with neuropsychological and psychopathological parameters. *Eur Arch Psychiatry Clin Neurosci.* 1992;241(6):328–332. doi:10.1007/BF02191956
13. Uhlhaas PJ, Singer W. Abnormal neural oscillations and synchrony in schizophrenia. *Nat Rev Neurosci.* 2010;11(2):100–113. doi:10.1038/nrn2774
14. McNally JM, McCarley RW. Gamma band oscillations: a key to understanding schizophrenia symptoms and neural circuit abnormalities. *Curr Opin Psychiatry* 2016;29(3):202–210. doi:10.1097/YCO.0000000000000244
15. Andreou C, Nolte G, Leicht G, et al. Increased resting-state gamma-band connectivity in first-episode schizophrenia. *Schizophr Bull.* 2015;41(4):930–939. doi:10.1093/schbul/sbu121
16. Grutzner C, Uhlhaas PJ, Genc E, Kohler A, Singer W, Wibral M. Neuroelectromagnetic correlates of perceptual closure processes. *J Neurosci.* 2010;30(24):8342–8352. doi:10.1523/JNEUROSCI.5434-09.2010
17. Grent-'t-Jong T, Rivolta D, Sauer A, et al. MEG-measured visually induced gamma-band oscillations in chronic schizophrenia: evidence for impaired generation of rhythmic activity in ventral stream regions. *Schizophr Res.* 2016;176(2-3):177–185. doi:10.1016/j.schres.2016.06.003
18. van der Vinne N, Vollebregt MA, van Putten MJAM, Arns M. Frontal alpha asymmetry as a diagnostic marker in depression: fact or fiction? A meta-analysis. *NeuroImage Clin.* 2017;16:79–87. doi:10.1016/j.nicl.2017.07.006

19. Stewart JL, Coan JA, Towers DN, Allen JJB. Frontal EEG asymmetry during emotional challenge differentiates individuals with and without lifetime major depressive disorder. *J Affect Disord.* 2011;129(1-3):167–174. doi:10.1016/j.jad.2010.08.029
20. Olbrich S, van Dinteren R, Arns M. Personalized medicine: review and perspectives of promising baseline EEG biomarkers in major depressive disorder and attention deficit hyperactivity disorder. *Neuropsychobiology* 2016;72(3-4):229–240. doi:10.1159/000437435
21. Mackintosh AJ, De Bock R, Lim Z, et al. Psychotic disorders, dopaminergic agents and EEG/MEG resting-state functional connectivity: a systematic review. *Neurosci Biobehav Rev.* 2021;120:354–371. doi:10.1016/j.neubiorev.2020.10.021
22. Gemein LAW, Schirrmeister RT, Chrabąszcz P, et al. Machine-learning-based diagnostics of EEG pathology. *Neuroimage* 2020;220:117021. doi:10.1016/j.neuroimage.2020.117021
23. Hosseini MP, Hosseini A, Ahi K. A review on machine learning for EEG signal processing in bioengineering. *IEEE Rev Biomed Eng.* 2021;14:204–218. doi:10.1109/RBME.2020.2969915
24. Chekroud AM, Bondar J, Delgadillo J, et al. The promise of machine learning in predicting treatment outcomes in psychiatry. *World Psychiatry* 2021;20(2):154–170. doi:10.1002/wps.20882
25. Woo CW, Chang LJ, Lindquist MA, Wager TD. Building better biomarkers: brain models in translational neuroimaging. *Nat Neurosci.* 2017;20(3):365–377. doi:10.1038/nn.4478
26. Barros C, Silva CA, Pinheiro AP. Advanced EEG-based learning approaches to predict schizophrenia: promises and pitfalls. *Artif Intell Med.* 2021;114:102039. doi:10.1016/j.artmed.2021.102039
27. Verma S, Goel T, Tanveer M, Ding W, Sharma R, Murugan R. Machine learning techniques for the schizophrenia diagnosis: a comprehensive review and future research directions. *J Ambient Intell Hum Comput.* 2023;14(5):4795–4807. doi:10.1007/s12652-023-04536-6
28. Safayari A, Bolhasani H. Depression diagnosis by deep learning using EEG signals: a systematic review. *Med Nov Technol Devices* 2021;12:100102. doi:10.1016/j.medntd.2021.100102
29. Gao S, Calhoun VD, Sui J. Machine learning in major depression: from classification to treatment outcome prediction. *CNS Neurosci Ther.* 2018;24(11):1037–1052. doi:10.1111/cns.13048
30. Khosla A, Khandnor P, Chand T. Automated diagnosis of depression from EEG signals using traditional and deep learning approaches: a comparative analysis. *Biocybern Biomed Eng.* 2022;42(1):108–142. doi:10.1016/j.bbe.2021.12.005
31. Jang KI, Kim S, Kim SY, Lee C, Chae JH. Machine learning-based electroencephalographic phenotypes of schizophrenia and major depressive disorder. *Front Psychiatry* 2021;12:745458. https://www.frontiersin.org/articles/10.3389/fpsyt.2021.745458. Accessed September 22, 2023.
32. Goshvarpour A, Goshvarpour A. Schizophrenia diagnosis using innovative EEG feature-level fusion schemes. *Phys Eng Sci Med.* 2020;43(1):227–238. doi:10.1007/s13246-019-00839-1
33. Li F, Wang J, Liao Y, et al. Differentiation of schizophrenia by combining the spatial EEG brain network patterns of rest and task P300. *IEEE Trans Neural Syst Rehabil Eng.* 2019;27(4):594–602. doi:10.1109/TNSRE.2019.2900725
34. Jahmunah V, Lih Oh S, Rajinikanth V, et al. Automated detection of schizophrenia using nonlinear signal processing methods. *Artif Intell Med.* 2019;100:101698. doi:10.1016/j.artmed.2019.07.006
35. Park SM, Jeong B, Oh DY, et al. Identification of major psychiatric disorders from resting-state electroencephalography using a machine learning approach. *Front Psychiatry* 2021;12:707581. https://www.frontiersin.org/articles/10.3389/fpsyt.2021.707581. Accessed December 10, 2023.
36. Khan DM, Yahya N, Kamel N, Faye I. Automated diagnosis of major depressive disorder using brain effective connectivity and 3D convolutional neural network. *IEEE Access.* 2021;9:8835–8846. doi:10.1109/ACCESS.2021.3049427
37. Yasin S, Hussain SA, Aslan S, Raza I, Muzammel M, Othmani A. EEG based major depressive disorder and bipolar disorder detection using neural networks:a review. *Comput Methods Programs Biomed.* 2021;202:106007. doi:10.1016/j.cmpb.2021.106007
38. Kinder I, Friganovic K, Vukojevic J, et al. Comparison of machine learning methods in classification of affective disorders. In: *2020 43rd International Convention on Information, Communication and Electronic Technology (MIPRO)*; 2020:177–181. doi:10.23919/MIPRO48935.2020.9245335
39. Emre IE, Erol C, Taş C, Tarhan N. Multi-class classification model for psychiatric disorder discrimination. *Int J Med Inf.* 2023;170:104926. doi:10.1016/j.ijmedinf.2022.104926
40. Shor O, Yaniv-Rosenfeld A, Valevski A, Weizman A, Khrennikov A, Benninger F. EEG-based spatio-temporal relation signatures for the diagnosis of depression and schizophrenia. *Sci Rep.* 2023;13(1):776. doi:10.1038/s41598-023-28009-0
41. Ying X. An overview of overfitting and its solutions. *J Phys Conf Ser.* 2019;1168(2):022022. doi:10.1088/1742-6596/1168/2/022022
42. Franke K, Ziegler G, Klöppel S, Gaser C; Alzheimer's Disease Neuroimaging Initiative. Estimating the age of healthy subjects from T1-weighted MRI scans using Kernel methods: exploring the influence of various parameters. *Neuroimage* 2010;50(3):883–892. doi:10.1016/j.neuroimage.2010.01.005
43. Schnack HG, van Haren NEM, Nieuwenhuis M, Hulshoff Pol HE, Cahn W, Kahn RS. Accelerated brain aging in schizophrenia: a longitudinal pattern recognition study. *Am J Psychiatry* 2016;173(6):607–616. doi:10.1176/appi.ajp.2015.15070922
44. Kaufmann T, van der Meer D, Doan NT, et al. Common brain disorders are associated with heritable patterns of apparent aging of the brain. *Nat Neurosci.* 2019;22(10):1617–1623. doi:10.1038/s41593-019-0471-7
45. Chung Y, Addington J, Bearden CE, et al. Use of machine learning to determine deviance in neuroanatomical maturity associated with future psychosis in youths at clinically high risk. *JAMA Psychiatry* 2018;75(9):960–968. doi:10.1001/jamapsychiatry.2018.1543
46. Hajek T, Franke K, Kolenic M, et al. Brain age in early stages of bipolar disorders or schizophrenia. *Schizophr Bull.* 2019;45(1):190–198. doi:10.1093/schbul/sbx172
47. Kolenic M, Franke K, Hlinka J, et al. Obesity, dyslipidemia and brain age in first-episode psychosis. *J Psychiatr Res.* 2018;99:151–158. doi:10.1016/j.jpsychires.2018.02.012
48. Koutsouleris N, Davatzikos C, Borgwardt S, et al. Accelerated brain aging in schizophrenia and beyond: a neuroanatomical marker of psychiatric disorders. *Schizophr Bull.* 2014;40(5):1140–1153. doi:10.1093/schbul/sbt142
49. McWhinney S, Kolenic M, Franke K, et al. Obesity as a risk factor for accelerated brain ageing in first-episode psychosis—a longitudinal study. *Schizophr Bull.* 2021;47(6):1772–1781. doi:10.1093/schbul/sbab064
50. Lee WH, Antoniades M, Schnack HG, Kahn RS, Frangou S. Brain age prediction in schizophrenia: does the choice of machine learning algorithm matter? *Psychiatry Res Neuroimaging* 2021;310:111270. doi:10.1016/j.pscychresns.2021.111270

51. Nenadić I, Dietzek M, Langbein K, Sauer H, Gaser C. BrainAGE score indicates accelerated brain aging in schizophrenia, but not bipolar disorder. *Psychiatry Res Neuroimaging* 2017;266:86–89. doi:10.1016/j.pscychresns.2017.05.006
52. Koutsouleris N, Pantelis C, Velakoulis D, et al. Exploring links between psychosis and frontotemporal dementia using multimodal machine learning: dementia praecox revisited. *JAMA Psychiatry* 2022;79(9):907–919. doi:10.1001/jamapsychiatry.2022.2075
53. Besteher B, Gaser C, Nenadić I. Machine-learning based brain age estimation in major depression showing no evidence of accelerated aging. *Psychiatry Res Neuroimaging* 2019;290:1–4. doi:10.1016/j.pscychresns.2019.06.001
54. Christman S, Bermudez C, Hao L, et al. Accelerated brain aging predicts impaired cognitive performance and greater disability in geriatric but not midlife adult depression. *Transl Psychiatry* 2020;10(1):317. doi:10.1038/s41398-020-01004-z
55. Han LKM, Dinga R, Hahn T, et al. Brain aging in major depressive disorder: results from the ENIGMA major depressive disorder working group. *Mol Psychiatry* 2021;26(9):5124–5139. doi:10.1038/s41380-020-0754-0
56. Han S, Chen Y, Zheng R, et al. The stage-specifically accelerated brain aging in never-treated first-episode patients with depression. *Hum Brain Mapp.* 2021;42(11):3656–3666. doi:10.1002/hbm.25460
57. Al Zoubi O, Ki Wong C, Kuplicki RT, et al. Predicting age from brain EEG signals—a machine learning approach. *Front Aging Neurosci.* 2018;10:184. doi:10.3389/fnagi.2018.00184
58. Sun H, Paixao L, Oliva JT, et al. Brain age from the electroencephalogram of sleep. *Neurobiol Aging* 2019;74:112–120. doi:10.1016/j.neurobiolaging.2018.10.016
59. Engemann DA, Mellot A, Höchenberger R, et al. A reusable benchmark of brain-age prediction from M/EEG resting-state signals. *Neuroimage.* 2022;262:119521. doi:10.1016/j.neuroimage.2022.119521
60. Dimitriadis SI, Salis CI. Mining time-resolved functional brain graphs to an EEG-based Chronnectomic Brain Aged Index (CBAI). *Front Hum Neurosci.* 2017;11:423. doi:10.3389/fnhum.2017.00423
61. Barry RJ, De Blasio FM. EEG differences between eyes-closed and eyes-open resting remain in healthy ageing. *Biol Psychol.* 2017;129:293–304. doi:10.1016/j.biopsycho.2017.09.010
62. Vlahou EL, Thurm F, Kolassa IT, Schlee W. Resting-state slow wave power, healthy aging and cognitive performance. *Sci Rep.* 2014;4(1):5101. doi:10.1038/srep05101
63. World Health Organization, ed. *The ICD-10 Classification of Mental and Behavioural Disorders: Diagnostic Criteria for Research*. Geneva: World Health Organization; 1993.
64. Declaration of Helsinki. Recommendations guiding medical doctors in biomedical research involving human subjects. *Ugeskr Laeger.* 1976;138(7):399–400.
65. American Electroencephalographic society guidelines for standard electrode position nomenclature. *J Clin Neurophysiol.* 1991;8(2):200–202. doi:10.1097/00004691-199104000-00007
66. Tadel F, Baillet S, Mosher JC, Pantazis D, Leahy RM. Brainstorm: a user-friendly application for MEG/EEG Analysis. *Comput Intel Neurosc*. 2011;2011:1–13. doi:10.1155/2011/879716
67. Cohen MX. *Analyzing Neural Time Series Data: Theory and Practice*. Cambridge, Massachusetts, United States: The MIT Press; 2014. doi:10.7551/mitpress/9609.001.0001
68. Welch P. The use of fast Fourier transform for the estimation of power spectra: a method based on time averaging over short, modified periodograms. *IEEE Trans Audio Electroacoust.* 1967;15(2):70–73. doi:10.1109/TAU.1967.1161901
69. McLntosh AR, Gonzalez-Lima F. Structural equation modeling and its application to network analysis in functional brain imaging. *Hum Brain Mapp.* 1994;2(1-2):2–22. doi:10.1002/hbm.460020104
70. Ruschhaupt M, Huber W, Poustka A, Mansmann U. A compendium to ensure computational reproducibility in high-dimensional classification tasks. *Stat Appl Genet Mol Biol.* 2004;3(1):1–24. doi:10.2202/1544-6115.1078
71. Koutsouleris N, Kahn RS, Chekroud AM, et al. Multisite prediction of 4-week and 52-week treatment outcomes in patients with first-episode psychosis: a machine learning approach. *Lancet Psychiatry*. 2016;3(10):935–946. doi:10.1016/S2215-0366(16)30171-7
72. Varma S, Simon R. Bias in error estimation when using cross-validation for model selection. *BMC Bioinf.* 2006;7(1):91. doi:10.1186/1471-2105-7-91
73. Filzmoser P, Liebmann B, Varmuza K. Repeated double cross validation. *J Chemom.* 2009;23(4):160–171. doi:10.1002/cem.1225
74. Dukart J, Schroeter ML, Mueller K; The Alzheimer's Disease Neuroimaging Initiative. Age correction in dementia – matching to a healthy brain. Valdes-Sosa PA, ed. *PLoS ONE.* 2011;6(7):e22193. doi:10.1371/journal.pone.0022193
75. Koutsouleris N, Meisenzahl EM, Borgwardt S, et al. Individualized differential diagnosis of schizophrenia and mood disorders using neuroanatomical biomarkers. *Brain.* 2015;138(7):2059–2073. doi:10.1093/brain/awv111
76. Leucht S, Samara M, Heres S, Patel MX, Woods SW, Davis JM. Dose equivalents for second-generation antipsychotics: the minimum effective dose method. *Schizophr Bull.* 2014;40(2):314–326. doi:10.1093/schbul/sbu001
77. Leucht S, Samara M, Heres S, et al. Dose equivalents for second-generation antipsychotic drugs: the classical mean dose method. *Schizophr Bull.* 2015;41(6):1397–1402. doi:10.1093/schbul/sbv037
78. Patel MX, Arista IA, Taylor M, Barnes TRE. How to compare doses of different antipsychotics: a systematic review of methods. *Schizophr Res.* 2013;149(1-3):141–148. doi:10.1016/j.schres.2013.06.030
79. Hayasaka Y, Purgato M, Magni LR, et al. Dose equivalents of antidepressants: evidence-based recommendations from randomized controlled trials. *J Affect Disord.* 2015;180:179–184. doi:10.1016/j.jad.2015.03.021
80. Pearson KX. On the criterion that a given system of deviations from the probable in the case of a correlated system of variables is such that it can be reasonably supposed to have arisen from random sampling. *Lond Edinb Dublin Philos Mag J Sci.* 1900;50(302):157–175. doi:10.1080/14786440009463897
81. Conover WJ. The rank transformation—an easy and intuitive way to connect many nonparametric methods to their parametric counterparts for seamless teaching introductory statistics courses. *WIREs Comput Stat.* 2012;4(5):432–438. doi:10.1002/wics.1216
82. Kruskal WH, Wallis WA. Use of ranks in one-criterion variance analysis. *J Am Stat Assoc.* 1952;47(260):583–621. doi:10.1080/01621459.1952.10483441
83. Dunn OJ. Multiple comparisons using rank sums. *Technometrics.* 1964;6(3):241–252. doi:10.1080/00401706.1964.10490181
84. Cole JH, Ritchie SJ, Bastin ME, et al. Brain age predicts mortality. *Mol Psychiatry.* 2018;23(5):1385–1392. doi:10.1038/mp.2017.62
85. Golland P, Fischl B. Permutation Tests for Classification: towards Statistical Significance in Image-Based Studies. In: Taylor C, Noble JA, eds. *Information Processing in Medical Imaging*. Vol 2732. Lecture Notes in Computer Science.

Berlin, Heidelberg: Springer Berlin Heidelberg; 2003:330–341. doi:10.1007/978-3-540-45087-0_28

86. Gómez-Verdejo V, Parrado-Hernández E, Tohka J; Alzheimer's Disease Neuroimaging Initiative. Sign-consistency based variable importance for machine learning in brain imaging. *Neuroinformatics*. 2019;17(4):593–609. doi:10.1007/s12021-019-9415-3
87. Koutsouleris N, Dwyer DB, Degenhardt F, et al. Multimodal machine learning workflows for prediction of psychosis in patients with clinical high-risk syndromes and recent-onset depression. *JAMA Psychiatry* 2021;78(2):195–209. doi:10.1001/jamapsychiatry.2020.3604
88. Farahani FV, Karwowski W, Lighthall NR. Application of graph theory for identifying connectivity patterns in human brain networks: a systematic review. *Front Neurosci.* 2019;13:585. https://www.frontiersin.org/articles/10.3389/fnins.2019.00585. Accessed April 27, 2023.
89. Lemere F. Effects on electroencephalogram of various agents used in treating schizophrenia. *J Neurophysiol.* 1938;1(6):590–595. doi:10.1152/jn.1938.1.6.590
90. Sponheim SR, Clementz BA, Iacono WG, Beiser M. Resting EEG in first-episode and chronic schizophrenia. *Psychophysiology* 1994;31(1):37–43. doi:10.1111/j.1469-8986.1994.tb01023.x
91. Clementz BA, Sponheim SR, Iacono WG, Beiser M. Resting EEG in first-episode schizophrenia patients, bipolar psychosis patients, and their first-degree relatives. *Psychophysiology* 1994;31(5):486–494. doi:10.1111/j.1469-8986.1994.tb01052.x
92. Merrin EL, Floyd TC. Negative symptoms and EEG alpha in schizophrenia: a replication. *Schizophr Res.* 1996;19(2-3):151–161. doi:10.1016/0920-9964(96)88522-7
93. Ramsay IS, Schallmo MP, Biagianti B, Fisher M, Vinogradov S, Sponheim SR. Deficits in auditory and visual sensory discrimination reflect a genetic liability for psychosis and predict disruptions in global cognitive functioning. *Front Psychiatry.* 2020;11:638. doi:10.3389/fpsyt.2020.00638
94. Ramsay IS, Pokorny VJ, Lynn PA, Klein SD, Sponheim SR. Limited consistency and strength of neural oscillations during sustained visual attention in schizophrenia. *Biol Psychiatry Cogn Neurosci Neuroimaging*. 2024;9(3):337–345. doi:10.1016/j.bpsc.2023.02.001
95. Ricceri L, Minghetti L, Moles A, et al. Cognitive and neurological deficits induced by early and prolonged basal forebrain cholinergic hypofunction in rats. *Exp Neurol.* 2004;189(1):162–172. doi:10.1016/j.expneurol.2004.05.025
96. Platt B, Riedel G. The cholinergic system, EEG and sleep. *Behav Brain Res.* 2011;221(2):499–504. doi:10.1016/j.bbr.2011.01.017
97. Schumacher J, Thomas AJ, Peraza LR, et al. EEG alpha reactivity and cholinergic system integrity in Lewy body dementia and Alzheimer's disease. *Alzheimers Res Ther*. 2020;12:46. doi:10.1186/s13195-020-00613-6
98. Higley MJ, Picciotto MR. Neuromodulation by acetylcholine: examples from schizophrenia and depression. *Curr Opin Neurobiol.* 2014;29:88–95. doi:10.1016/j.conb.2014.06.004
99. Scarr E, Gibbons A, Neo J, Udawela M, Dean B. Cholinergic connectivity: it's implications for psychiatric disorders. *Front Cell Neurosci.* 2013;7:55. https://www.frontiersin.org/articles/10.3389/fncel.2013.00055. Accessed April 10, 2023.
100. Smart OL, Tiruvadi VR, Mayberg HS. Multimodal Approaches to Define Network Oscillations in Depression. *Biol Psychiatry* 2015;77(12):1061–1070. doi:10.1016/j.biopsych.2015.01.002
101. Allen JJB, Urry HL, Hitt SK, Coan JA. The stability of resting frontal electroencephalographic asymmetry in depression. *Psychophysiology* 2004;41(2):269–280. doi:10.1111/j.1469-8986.2003.00149.x
102. Jaspers K. *Allgemeine Psychopathologie. 9. unveränderte Aufl.* Berlin Heidelberg, New-York: Springer; 1973.
103. Ellison-Wright I, Bullmore E. Anatomy of bipolar disorder and schizophrenia: a meta-analysis. *Schizophr Res.* 2010;117(1):1–12. doi:10.1016/j.schres.2009.12.022
104. Leirer VM, Wienbruch C, Kolassa S, Schlee W, Elbert T, Kolassa IT. Changes in cortical slow wave activity in healthy aging. *Brain Imaging Behav*. 2011;5(3):222–228. doi:10.1007/s11682-011-9126-3
105. Finnigan S, Robertson IH. Resting EEG theta power correlates with cognitive performance in healthy older adults. *Psychophysiology.* 2011;48(8):1083–1087. doi:10.1111/j.1469-8986.2010.01173.x
106. Fenton GW, Fenwick PBC, Dollimore J, Dunn TL, Hirsch SR. Eeg spectral analysis in schizophrenia. *Br J Psychiatry.* 1980;136(5):445–455. doi:10.1192/bjp.136.5.445
107. Jabès A, Klencklen G, Ruggeri P, Antonietti JP, Banta Lavenex P, Lavenex P. Age-related differences in resting-state EEG and allocentric spatial working memory performance. *Front Aging Neurosci.* 2021;13:704362. doi:10.3389/fnagi.2021.704362
108. Rossini PM, Rossi S, Babiloni C, Polich J. Clinical neurophysiology of aging brain: from normal aging to neurodegeneration. *Prog Neurobiol.* 2007;83(6):375–400. doi:10.1016/j.pneurobio.2007.07.010
109. Babiloni C, Binetti G, Cassarino A, et al. Sources of cortical rhythms in adults during physiological aging: a multicentric EEG study. *Hum Brain Mapp.* 2005;27(2):162–172. doi:10.1002/hbm.20175
110. Perinelli A, Assecondi S, Tagliabue CF, Mazza V. Power shift and connectivity changes in healthy aging during resting-state EEG. *Neuroimage* 2022;256:119247. doi:10.1016/j.neuroimage.2022.119247
111. Franke K, Gaser C. Ten Years of BrainAGE as a neuroimaging biomarker of brain aging: what insights have we gained? *Front Neurol.* 2019;10:789. doi:10.3389/fneur.2019.00789
112. Franke K, Bublak P, Hoyer D, et al. In vivo biomarkers of structural and functional brain development and aging in humans. *Neurosci Biobehav Rev.* 2020;117:142–164. doi:10.1016/j.neubiorev.2017.11.002
113. Sapolsky RM, Krey LC, McEwen BS. The neuroendocrinology of stress and aging: the glucocorticoid cascade hypothesis. *Sci Aging Knowl Environ*. 2002;2002(38):cp21. doi:10.1126/sageke.2002.38.cp21
114. Klippel A, Viechtbauer W, Reininghaus U, et al. The cascade of stress: a network approach to explore differential dynamics in populations varying in risk for psychosis. *Schizophr Bull.* 2018;44(2):328–337. doi:10.1093/schbul/sbx037
115. Bersani FS, Mellon SH, Reus VI, Wolkowitz OM. Accelerated aging in serious mental disorders. *Curr Opin Psychiatry* 2019;32(5):381–387. doi:10.1097/YCO.0000000000000525
116. Nguyen TT, Eyler LT, Jeste DV. Systemic Biomarkers of Accelerated Aging in Schizophrenia: a critical review and future directions. *Schizophr Bull.* 2018;44(2):398–408. doi:10.1093/schbul/sbx069
117. Olabi B, Ellison-Wright I, McIntosh AM, Wood SJ, Bullmore E, Lawrie SM. Are there progressive brain changes in schizophrenia? A meta-analysis of structural magnetic resonance imaging studies. *Biol Psychiatry* 2011;70(1):88–96. doi:10.1016/j.biopsych.2011.01.032
118. Lieslehto J, Jääskeläinen E, Kiviniemi V, et al. The progression of disorder-specific brain pattern expression in schizophrenia over 9 years. *npj Schizophr.* 2021;7:32. doi:10.1038/s41537-021-00157-0